Angewandte Chemie
GDCh
Eine Zeitschrift der Gesellschaft Deutscher Chemiker
www.angewandte.de

Akzeptierter Artikel

Titel: Scalable, Durable, and Recyclable Metal-Free Catalysts for Highly-Efficient Conversion of CO2 to Cyclic Carbonates

Autoren: Yao-Yao Zhang, Guan-Wen Yang, Rui Xie, Li Yang, Bo Li, and Guang-Peng Wu

Zitierweise: *Angew. Chem. Int. Ed.* 10.1002/anie.202010651

Link zur VoR: https://doi.org/10.1002/anie.202010651

WILEY-VCH

Scalable, Durable, and Recyclable Metal-Free Catalysts for Highly-Efficient Conversion of CO_2 to Cyclic Carbonates

Yao-Yao Zhang,[a] Guan-Wen Yang,[a] Rui Xie,[a] Li Yang,[a] Bo Li,[b] and Guang-Peng Wu*[a]

[a] Y.-Y. Zhang, G.-W. Yang, R. Xie, L. Yang, Prof. Dr. G.-P. Wu
MOE Laboratory of Macromolecular Synthesis and Functionalization, Adsorption and Separation Materials and Technologies of Zhejiang Province,
Department of Polymer Science and Engineering
Zhejiang University
Zhe Da Road 38, Hangzhou 310027, China
E-mail: gpwu@zju.edu.cn
[b] Prof. B. Li
College of Material, Chemistry and Chemical Engineering
Hangzhou Normal University
Yuhangtang Road 2318, Hangzhou 311121, China

Supporting information for this article is given via a link at the end of the document.

Abstract: This article communicates a series of highly active organoboron catalysts for coupling of CO_2 and epoxides with merits of scalable preparation, thermostability, and recyclability. The metal-free catalysts show high reactivity towards a wide scope of cyclic carbonates (14 examples) and can withstand a high temperature up to 150 °C. Compared with most of the current metal-free catalytic systems involved using mol% catalyst loading, the catalytic capacity of our catalyst can be enhanced by three orders of magnitude (epoxide/cat. = 200,000/1, mole ratio) in the presence of cocatalyst, which greatly narrows the gap between the metal-free catalysts and state-of-the-art metallic systems. An intramolecular cooperative mechanism is proposed and certified on the basis of investigations on crystal structures, structure-performance relationship, kinetic studies, and key reaction intermediates.

Introduction

The runaway greenhouse effect and the resultant dangerous climate change urgently require efficient techniques for chemical transformation of CO_2 into value-added products. Among many efforts on catalytic transformation of this abundant C1 feedstock,[1] the coupling of CO_2 and epoxides into cyclic and polymeric carbonates stands out as a great choice because of its atom-economic merit and high carbon fixation (Scheme 1). Furthermore, compared to the hottest redox transformation CO_2 into methanol, syngas, and light alkenes that inevitably involved with harsh conditions,[2] the coupling of CO_2 and epoxides into cyclic and polymeric carbonates could be performed at rather mild reaction conditions, even at normal temperature and pressure in the presence of an efficient catalyst.[3] Currently, considerable attentions are being paid to the CO_2-based polycarbonates, but the cyclic counterparts have been proved to be more useful, which are widely utilized in polar aprotic solvents,[4] electrolytes for lithium-ion battery,[5] raw materials in aromatic polycarbonate,[6] and pharmaceutical intermediates (Scheme 1).[7] In the past decades, numerous robust metallic catalysts have been developed for cyclization of CO_2 and epoxides.[3, 8] Despite the fact that significant advances were achieved, the time-consuming multistep synthesis of these organometallic catalysts remains key challenge, such as salen and porphyrin metal complexes.

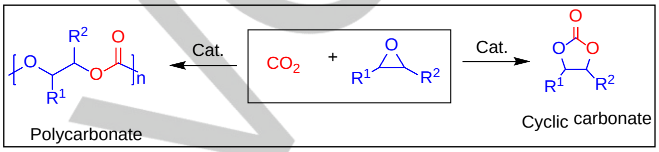

Scheme 1. The coupling reaction of CO_2 and epoxide.

Recently, metal-free catalytic systems gain momentum due to their versatile chemical structure, simplified preparation procedure, and avoidance of metal removal.[9] A number of catalysts, including imidazolium salts,[10] quaternary ammonium salts,[11] phosphonium salts,[12] amidine-based,[13] carbene-based,[14] and hydrogen bond donor-based[15] catalytic systems have been widely investigated for coupling CO_2 with epoxides. On the other hand, even though the heterogeneous catalytic systems can be easily separated from products for reuse,[16] the investigation of homogeneous compounds is necessary in clarification of structure−performance relationship, which is beneficial to the insightful understanding of the reaction mechanism and the subsequent design of more advanced catalytic systems. Given that a vast number of organic systems have been venturing into this field, several representative systems are selected and presented here. In 2017, Kleij *et al.* described a squaramides/quaternary ammonium salt catalytic system.[15b] With the assistant of the squaramides in activating epoxide, the catalyst displays quite high activity for conversion of hexene epoxide with epoxide/catalyst ratio of 50/1 under 80 °C, 10 bar [turnover frequency (TOF) = 85 h^{-1}]. The same group also reported that usage of cavitand-based polyphenols combining with tetrabutylammonium iodide (TBAI) shows an outstanding reactivity towards cyclic hexene carbonate with a TOF value of 488 h^{-1}.[15i] North and coworkers demonstrated that the halid-free Salophen ligand could effectively transform epoxides into cyclic carbonates at 120 °C and 5 bar CO_2 pressure with epoxide/catalyst ratio of 100/1, giving a 94 % conversion of 3-phenoxypropylene oxide in 3.5 h.[15h] Besides, one more challenging task for these organic catalysts is how to effectively transform epoxides to cyclic carbonates at ambient condition, an admirable environmental-friendly and carbon-balance approach for CO_2 conversion.[3e] Facing this challenge, Zhang recently reported a series of protic ionic liquids for cycloaddition of CO_2 to epoxide under mild condition with a TOF up to 2.6 h^{-1} at catalyst loading of 6 mol% using epichlorohydrin as the substrate.[13b] Lu and Zhou described kinds of phosphorus ylide CO_2 adducts that were able to effectively catalyze the conversion of terminal epoxides and CO_2 into cyclic carbonates under ambient conditions, and an unprecedented TOF value (3.6 h^{-1}) of propylene oxide (PO) was achieved at a PO/catalyst ratio of 20/1.[12g] Despite the fact that the activity for these metal-free system cannot compete with the state-of-the-art metallic compounds, these well-defined chemical structures and the insightful mechanistic investigations shed light on further metal-free catalyst design.

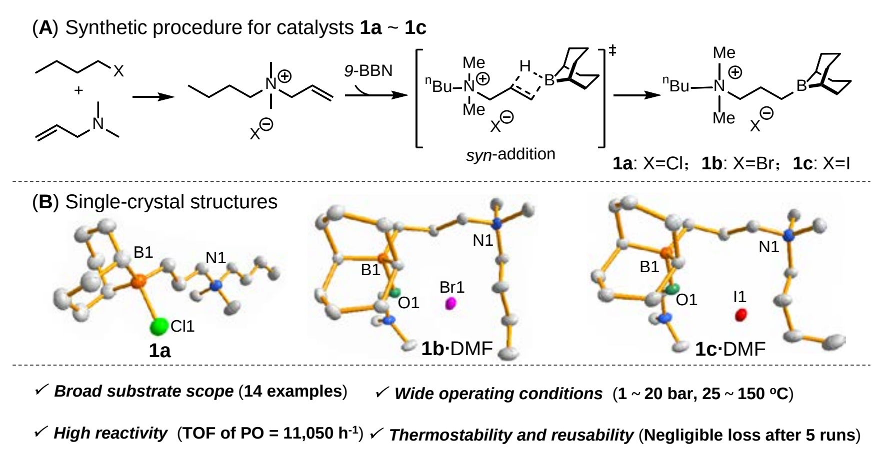

Figure 1. (A) Synthetic procedure of organoboron catalysts **1a**~**1c**. (B) Single-crystal structures of catalysts **1a**, **1b**·DMF, and **1c**·DMF at the 50 % probability level**.** All hydrogen atoms were omitted for clarity. The data for the X-ray crystallographic structure have been deposited in the Cambridge Crystallographic Data Center under accession numbers CCDC: 2001552, 2001553, and 2001554.

More recently, we communicated a series of organoboron catalysts for copolymerization of CO_2 and internal epoxides [e.g., cyclohexene oxide (CHO)] with merits of unprecedented reactivity and scalable preparation.[17] An efficiency of 5.0 kg CO_2-polymer/g catalyst was achieved, which is the highest record achieved to date in all of homogeneous organic and metallic catalysts for the CHO/CO_2 coupling reaction. Interestingly, by adding one more alkylborane center into the catalyst structure, the binuclear boron compounds show unprecedented activity for ring-opening polymerization of epoxides.[18] In addition, the synthetic procedure for these catalysts is extremely simple and efficient, the scalable preparation of these catalysts could be performed on a kilogram scale with nearly quantitative yield via two steps using commercially available stocks.

To broaden the range of applications for these metal-free catalysts, herein, we show our efforts on coupling of epoxides with CO_2 into various cyclic carbonates that are widely utilized in fine chemicals and polymer precursors. We found these catalysts show comparable reactivity to the metal-based catalysts towards a wide scope of cyclic carbonates and can withstand a high temperature up to 150 °C. Compared with other metal-free catalysts reported so far, the catalyst **1c** achieves the highest activity for coupling of PO/CO_2 both at optimized condition (TOF = 11,050 h^{-1}, 150 °C, and 10 bar) and ambient condition (TOF = 4.0 h^{-1}, 25 °C, and 1 bar), rendering our organoboron catalyst to be one of the most efficient metal-free catalytic systems. Catalyst recycling studies showed negligible loss in catalytic activity after five batch catalytic runs; while over 99% product selectivity was remained. The structure-performance relationship of our catalyst was systematically investigated by tuning the electronic and steric properties on the boron center (electrophilic site) and the quaternary ammonium salt (nucleophilic site), as well as the distance between electrophilic and nucleophilic centers. Lastly, a detailed catalytic cycle was proposed on the basis of the kinetic studies and key intermediates in the coupling reaction.

Results and Discussion

Synthesis and characterization of organoboron catalysts. The synthetic procedure of our bifunctional organoboron catalysts **1a**, **1b**, and **1c** are presented in Figure 1A, wherein two-step synthetic process with a nearly quantitative yield is applied.[17,18] The reaction of amine and alkyl halide (or alkenyl halide) generated allyl-containing quaternary ammonium salts, which sequentially produced the target catalysts **1a**, **1b**, and **1c** through the hydroboration reaction with borabicyclo[3.3.1]nonane (9-BBN) via regioselective *anti*-Markovnikov *syn*-addition. Benefited from the simple operation and nearly quantitative yield, the catalysts can be prepared on >1 kg scale as exemplified by **1c** in Figure S1.

The prepared catalysts were well characterized using single-crystal X-ray diffraction (SC-XRD) and nuclear magnetic resonance (NMR) (Supporting information), and the crystal structures of **1a**, **1b**, and **1c** are shown in Figure 1B. As observed from the stable solid structure of **1a**, the Cl^- coordinates to the boron atom with a Cl···B distance of 2.054(3) Å due to the electron-deficient property of boron center and the strong nucleophilicity of Cl^-. Being different with **1a** that is easy to crystallize in non-coordinating solvents (chloroform/hexane), it was rather difficult to get suitable crystals of **1b** and **1c** from the same solvents. The cultivation of crystals of **1b** and **1c** were conducted in a *N*,*N*-dimethylformamide (DMF) solution, respectively. These crystal structures were provided in Figure 1B, wherein one DMF molecule coordinated to the boron atom in **1b** and **1c** with O···B distances of 1.623(4) and 1.615(4) Å, respectively. In the solid structures of **1b** and **1c**, the anions are jointly trapped by the ammonium cation (N^+) and boron center (B), as observed by the Br^-···B and the Br^-···N distances of 6.018 and 5.404 Å, as well as the I^-···B and the I^-···N distances of 6.186 and 5.388 Å, respectively. Since the Br^- and I^- have lager radii and better leaving ability of I^- in compared with the Cl^- in **1a**, we can anticipate that the anions of Br^- and I^- in **1b** and **1c** would dynamically shuttle between the electron-deficient boron center and electropositive N^+ in non-coordinating solvent respectively; and this dynamic intramolecular structure has laid a foundation for the high activity of our catalysts for coupling of epoxides and CO_2, which is discussed in follows.

Catalytic performance. The screening experimental results for the CO_2/PO coupling reaction are summarized in Table 1, and the results in entries 1-3 reveal that the nucleophilic halide anion on catalyst significantly impacts the performance for cyclic carbonate formation. **1c** bearing I^{-} is the most effective catalyst, as witnessed by TOF values of 136 h^{-1} (**1a**, Cl^{-}), 192 h^{-1} (**1b**, Br^{-}), and 257 h^{-1} (**1c**, I^{-}) towards propylene carbonate (PC) under 80 °C and 20 bar of CO$_2$ with catalyst/PO ratio of 1/2,000. This observation was very different from the reactivity trend in the coupling of CHO with CO$_2$, where the polymerization activity order is Br^{-} > Cl^{-} > I^{-}.[17] The high activity for **1c** bearing I^{-} could be well explained by the following two facts. First, I^{-} has the largest radius compared with Cl^{-} and Br^{-}, and, in this case, the I^{-} is hard to coordinate to the electron-defect boron center, thereby the epoxide substrate would be more likely to be activated by complexation with the Lewis acidic boron center.[15b,19] The second factor is the good leaving ability of I^{-}, which could contribute to facilitating the formation of the thermally stable cyclic carbonate via backbiting reaction.[8j]

Table 1. Results for the coupling of PO and CO$_2$ catalyzed by organoboron catalysts.[a]

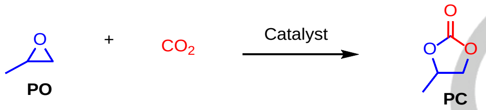

Entry	Catalyst (mol %)	Cat./PO (mol ratio)	Pressure (bar)	Temperature (°C)	Time (h)	Conversion (%)[b]	TOF (h^{-1})	Selectivity (%)[c]
1	**1a**	1/2,000	20	80	2	13.6	136	> 99
2	**1b**	1/2,000	20	80	2	19.2	192	> 99
3	**1c**	1/2,000	20	80	2	25.7	257	> 99
4	**1c**	1/2,000	20	90	2	28.5	285	> 99
5	**1c**	1/2,000	20	100	2	36.0	360	> 99
6	**1c**	1/2,000	20	120	2	44.6	446	> 99
7	**1c**	1/2,000	20	150	2	43.4	434	> 99
8	**1c**	1/2,000	5	120	2	43.6	436	> 99
9	**1c**	1/2,000	10	120	2	43.9	439	> 99
10	**1c**	1/2,000	15	120	2	44.3	443	> 99
11	**1c**	1/5,000	20	120	2	32.6	815	> 99
12[d]	**1c**	1/10,000	10	120	1	44.2	4420[e]	> 99
13[d]	**1c**	1/50,000	10	150	1	22.1	11050[f]	> 99
14[d]	**1c**	1/100,000	10	150	1	10.9	10900[g]	> 99
15	**1c**	1/500	20	25	16	>99.9	31.2	> 99
16	**1c**	1/100	1[h]	25	8	32.0	4.0	> 99

[a] All the reactions were carried out in 50 mL autoclaves in bulk. [b] The conversion of the PO was average of three runs. [c] The selectivity was determined by ^{1}H NMR. [d] 120 equivalents of TBAI to **1c** was used as the cocatalyst. In consideration of the catalytic ability of TBAI, the TOF values were respectively corrected as [e] 2360 h^{-1}, [f] 6950 h^{-1}, and [g] 6900 h^{-1} by eliminating the contribution of TBAI alone. [h] Using CO$_2$ balloon.

Owing to the high activity of complex **1c**, we selected it as the model catalyst to probe the effects of reaction pressure and temperature on the formation of cyclic carbonate with a **1c**/PO ratio of 1/2,000. An increase in the reaction temperature from 80 to 90, 100, and 120 °C resulted in a significant improvement in the catalytic activity and the TOFs increased from 257 h^{-1} to 285 h^{-1}, 360 h^{-1}, and 446 h^{-1}, respectively (Table 1, entries 3–6). The catalyst can stand high temperature up to 150 °C without evident loss in activity (Table 1, entry 7). The unconspicuous improvement at 150 °C could be attributed to the temperature-determined balance of the PO substrate in gas phase and liquid phase. Then the effect of CO$_2$ pressure was investigated at 120 °C, and the results indicated that the conversion of PO varied a little with the increase of CO$_2$ pressure from 5 to 20 bar (Table 1, entries 6, and 8–10). To our delight, even the catalyst loading reduced to 0.02 mol% (entry 11), TOF value achieved 815 h^{-1}. We further reduced the **1c** loading to 1/10,000 and 1/50,000 (**1c**/PO mole ratio, entries 12 and 13), with the assistance of TBAI, the coupling reaction can proceed smoothly and provided a reactivity of TOF up to 11,050 h^{-1}. To the best of our knowledge, the highest record value of the metal-free catalyst-mediated coupling of PO and CO$_2$ to date. When carrying out the catalysis with **1c**/PO=1/100,000 at 150 °C (entry 14), the catalyst remains highly active as the TOF value (10,900 h^{-1}) showing negligible decrease at such a diluted concentration of **1c**. Compared with most of the current metal-free systems involved using mol% catalyst loading, the catalytic ability of our catalyst was enhanced by three orders of magnitude (**1c**/PO = 1/100,000, mole ratio). These performances greatly narrow the gap between the metal-free catalysts and state-of-the-art metallic systems, and in some cases show comparability to metallic compounds (the comparison of **1c** with selected outstanding catalysts was provided in Scheme S1 and Table S4).[8b,8k,8o,8p,8q]

As above mentioned, the catalysts that are efficient under mild conditions are highly desirable. Consequently, we initially assessed the performance of **1c** at PO/**1c** ratio of 500/1 at room temperature (25 °C) under 20 bar CO$_2$ pressure and found that the substrate could be completely transformed into the cyclic carbonate in 16 h (Table 1, entry 15). This result drives us to perform the reaction at the most challenging conditions, *i.e.*, at room temperature and ordinary pressure (1 bar). It was a delight to find that even with [PO]/[**1c**] = 100/1, catalyst **1c** holds high reactivity for coupling of PO/CO$_2$, giving an admirable TOF value of 4.0 h^{-1} (Table 1, entry 16), as far as we know, the highest activity among all the homogeneous metal-free catalytic systems under a condition of normal pressure and temperature. The detailed comparison of **1c** with the other reported high-active metal-free catalytic systems is provided in Scheme S2 and Table S5.

Reusability of **1c** was also investigated in viewpoint of green chemistry. The coupling reaction of PO/CO_2 was first run in neat PO with [PO]/[**1c**] = 250/1 at 25 °C and 20 bar of CO_2 for 8 h; then the catalyst was recycled after distillation of the liquid product (100 °C, 3 torr). Benefit from its heat-resistant merit, the catalyst could be recycled at least 5 times. The results of five reaction cycles are shown in Figure S2, where no significant loss in reactivity was noted.

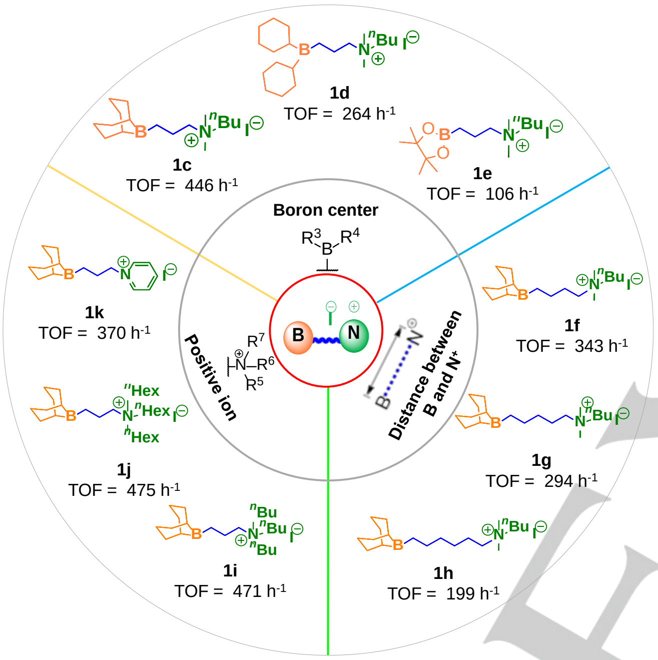

Figure 2. Systematical study on structure-activity relationships of the bifunctional catalysts. The TOF values of these catalysts are determined at 120 °C and 20 bar of CO_2 in 2 h with [PO]/[**1c**] = 2,000/1.

Structure optimization. Based on the inspiring catalytic results shown above and the block-based design of our catalysts, we were setting out to systematically study the structure-activity relationships by manipulating the steric and electronic substituents on the B and N atoms, as well as the linker length between the boron center and the ammonium cation (Figure 2). The conversion of PO at 120 °C and 20 bar of CO_2 in 2 h with 0.05 mol% catalyst loading was employed as the benchmark.

At first, we studied the electronic and steric effects on the boron atom (Figure 2, **1c**~**1e**). Compared with **1c** bearing BBN structure (TOF = 446 h^{-1}), catalyst **1d** bearing more steric but similar electrophilic cyclohexyl groups (BCy_2) shows retarded reactivity with a TOF value of 264 h^{-1}; when using catalyst **1e** that possesses the less steric and electrophilic 4,4,5,5-tetramethyl-1,2,2-dioxyl substituent (BPin), a much lower catalytic rate was observed (TOF = 106 h^{-1}). These results demonstrate that both the electronic and steric properties have great influence on the reactivity.

Increasing the linker length between the boron center and the ammonium cation has a negative effect on the coupling reaction (see catalysts **1c** and **1f**~**1h**, Figure 2). When the linker length increases from three to six methylene linkages, the TOF value dramatically decreased from 446 h^{-1} (by **1c**) to 343 h^{-1} (by **1f**), 294 h^{-1} (by **1g**), and 199 h^{-1} (by **1h**). Notably, this result was quite different with the copolymerization of CHO and CO_2, wherein the best performance was observed for a catalyst with a linker of pentamethylene.[17] We tentatively attributed this different trend to the steric demands on both of the reaction substrates (CHO vs PO) and reaction processes (polymerization vs cyclization).

The electronic and steric effects on nucleophilic motif were investigated by changing the substituents on the N atom (Figure 2, **1c** and **1i**~**1k**). We found that the larger steric hindrance groups on N atom can help to improve the reactivity of the coupling reaction. For example, compared to **1c** containing $Me_2{}^nBuN^+$ with a TOF value of 446 h^{-1}, catalysts **1i** bearing $^nBu_3N^+$ group and **1j** possessing $^nHex_3N^+$ group gave higher TOFs of 471 and 475 h^{-1}, respectively. This improvement of the reactivity can be attributed to the weakened interaction between the N^+ and I^-; in this context, the nucleophilic attack of I^- to the epoxide was reinforced, thereby the reactivity was promoted. This hypothesis was experimentally supported by the observation that the catalyst **1k** contains aromatic pyridinium and displayed a compromised catalytic activity of a TOF of 370 h^{-1} because of the enhanced electrostatic interaction between I^- and the pyridinium cation. All these results manifested that the electrophilic site, nucleophilic center, and linker length in the bifunctional catalysts are of vital importance in tuning the catalytic activity in cycloaddition of CO_2 with epoxides.

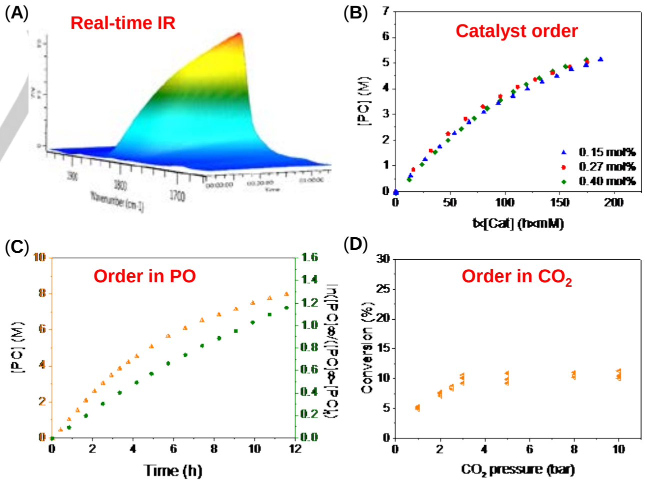

Figure 3. Kinetic measurements. (A) IR spectra monitoring formation of PC catalyzed by **1c**. Reaction orders in (B) catalyst, (C) PO, and (D) CO_2. The concentration of PC was calculated from the absorbance using the calibration curve (Figures S3 and S4).

Kinetic studies. To gather in-depth comprehension on the catalytic mechanism, kinetic measurements were first conducted to determine the order of each component using the model PO/CO_2 coupling reaction under **1c**. Real-time IR spectroscopy was used to monitor the reaction process based on the signal of the generated carbonyl group $\nu_{C=O}$ at 1,805 cm^{-1} of PC. A representative three-dimensional plot of IR spectrum was provided in Figure 3A, which shows an emergence and growth of the carbonyl stretch of PC. No characteristic signal of polycarbonate at 1,750 cm^{-1} appeared in each reaction. This experimental phenomenon excludes the possibility of the formation of PC through the depolymerization of the resultant polymers that usually occurs in the metal-catalyzed CO_2/PO coupling reactions.[20]

A first-order kinetic dependence on **1c** was observed by varying **1c** concentrations at 25 °C in neat PO and 20 bar of CO_2 [21] (Figures 3B and S5). The first-order in **1c** reveals that an intramolecular cooperating catalysis governed the coupling reaction of CO_2 and PO. Secondly, a first-order dependence on [PO] was also observed at 0.2 mol% catalyst loading by maintaining the CO_2 at 20 bar (Figure 3C). Then, we found that the coupling rate is independent in the range of 3 to 10 bar of CO_2 pressure, as evidenced by the initial rate of PC formation was almost constant with varied CO_2 pressure (Figure 3D). For accuracy, each experiment was carried out for three runs (Figure 3D). The low conversions at 1-3 bar of CO_2 pressure could be attributed to the limited CO_2 diffusion rate. The first order in [PO] and zero order in CO_2 pressure demonstrated that the ring-opening of the epoxide is the rate-determining step rather than the CO_2 insertion in the coupling reaction. The total activation energy was determined as 12.11 kcal/mol using Arrhenius equation (Figure S6), and such low activation energy also demonstrates the rationality of the high performance for our catalyst.

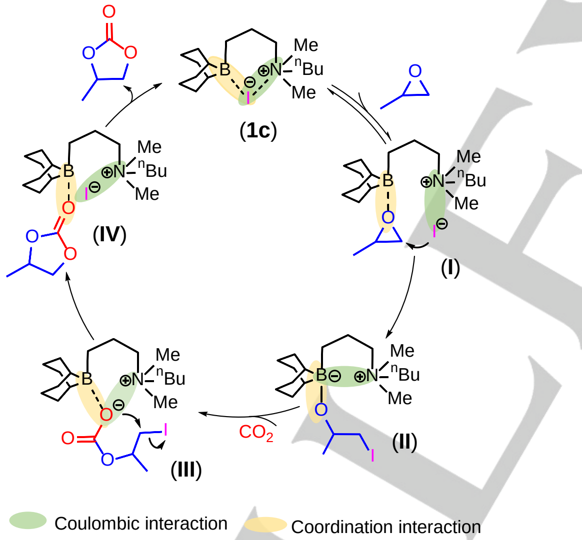

Scheme 2. The proposed mechanistic cycle for the coupling of PO with CO_2 based on **1c**.

Proposed mechanism. A catalytic cycle (Scheme 2) was proposed for **1c**-catalyzed CO_2/PO coupling reaction on the basis of the above kinetic studies and a deuterium labelling experiment (Figures S7-S9). As demonstrated in Scheme 2, the I^- in **1c** is co-trapped by a weak coordination with boron center and a Coulombic interaction with the ammonium cation. Benefiting from the weak interaction of I^- with boron center, the added PO can easily coordinate to the electrophilic boron center and afford an intermediate **I**. Subsequently, the coordinated PO undergoes a nucleophilic attack by the trapped I^- at the less steric site and generates intermediate **II**. Then, a CO_2 molecule immediately inserts into the boron-alkoxide bond to form a boron-carbonate species **III**. With the assistant of the electropositive quaternary ammonium, the intramolecular nucleophilic attack of carbonate on its methylene carbon produces the five-membered PC **IV**.[17] After release of PC, the catalyst is regenerated and the catalysis continues in the same way.

To support the proposed catalytic process, the intermediates at each step were identified and shown in Figure 4. First of all, **1c** was characterized by ^{11}B NMR spectrum, where a broad singlet at 87.58 ppm with a full width at half max (fwhm) of 841 Hz was observed (Figure 4a), which was approximately 0.53 ppm upfield shifted compared with the corresponding signal in *n*-hexyl-9-BBN (88.11 ppm, fwhm = 290 Hz, Figure S10). This observation confirmed the presence of a weak interaction between I^- and boron center in **1c**, as demonstrated at the beginning part of solid structure analysis.

Given the intermediate (**I**) in scheme 2 could not be directly detected because PO was ring-opened during the NMR measurement. In this context, 2-butene oxide was used due to its similar electronic effect with PO and its low reactivity under ambient temperature. The corresponding ^{11}B NMR spectrum in Figure 4b shows a singlet at 86.58 ppm with a fwhm of 817 Hz, a higher field shift of 1.00 ppm than that of **1c** (at 87.58 ppm), which indicates an existence of the weak coordination of the epoxide to the boron center.

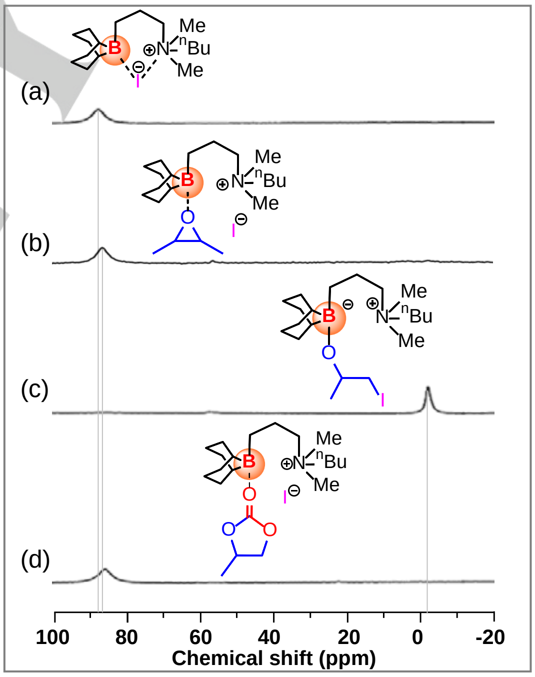

Figure 4. ^{11}B NMR spectra of catalytic intermediates. (a) **1c**, (b) **1c**/2-butene oxide (1/10 mole ratio), (c) **1c**/PO (1/10 mole ratio), and (d) **1c**/PC (1/10 mole ratio) in CD_2Cl_2, 192 MHz, 25 °C.

The direct evidence for the ring-opening of PO by **1c** (**1c**/PO = 1/10, mole ratio) was provided in Figure 4c, wherein a strong and sharp boron nucleus resonance at -1.32 ppm (fwhm = 317 Hz) was clearly observed, which could verify that the intermediate of **II** involved a tetra-coordinated boron structure.[22] The nucleophilic attack of **1c** at less steric site of PO was confirmed by the detection of the corresponding resultant iodoalcohol (Figure S11).

We were devoted to isolating and identifying the alkylboron-carbonate complex **III** shown in Scheme 2. However, our attempt to isolate the intermediate **III** was unsuccessful, because the cyclization reaction (i.e., from **II** to **IV**) was too fast even at low reaction temperature. Therefore, we were trying to characterize another boron-carbonate intermediate that could be regarded as an analogue to **III** but could not undergo cyclization reaction, thereby could be monitored by IR. In this context, we initially prepared a compound **II'** (Figure S12 in Supporting information) to simulate the intermediate **II**. Compared with the intermediate **II** (I^- is the counterion), the **II'** has a MeO^- as the counterion. In this regard, a boron-carbonate species (**III'**) with a $MeOCOO^-$ anion could be formed when the **II'** came in contact with CO_2. As expected, the generation of the **III'** was immediately formed after addition of CO_2 to **II'**. This process was monitored by Real-time IR spectroscopy (Figure S13), because the formed $MeOCOO^-$ anion could not undergo cyclization reaction. This control experiment in part support the intermediate of **III** in Scheme 2.

The evidence for the last intermediate (**IV**) proposed in the catalytic cycle in Scheme 2 was provided in Figure 4d. A weak interaction of PC with **1c** (10/1, mole ratio) was detected, wherein a broad resonance (fwhm = 897 Hz) at 85.76 ppm was observed. This weak interaction between the PC and catalyst should be beneficial for the regeneration of catalyst **1c**, thereby guaranteeing the smooth progress of the coupling reaction. In short, the identification of these intermediates provides solid support for the proposed mechanism; meanwhile the related ^{11}B NMR investigations give a rational explanation of the high reactivity of our catalysts for coupling of epoxides and CO_2.

Catalytic activity towards other epoxides. To test the scope of viable substrates for this reaction, various epoxides were investigated for the cyclization reaction with CO_2, wherein high reactivity and >99% product selectivity were observed for all the test substrates (Figure 5). Firstly, 1,2-epoxyalkanes with varying chain lengths (PO, ethylene oxide, butylene oxide, and hexene oxide) were effectively transformed to corresponding cyclic carbonates (**2a**, **2b**, **2c**, and **2d**) at [substrate]/[catalyst] ratio of 1,000/1) with high reactivity regardless of their steric bulk. The cycloaddition of CO_2 and epoxides with electron-withdrawing substitute were also tested. The result revealed that when using epichlorohydrin as the substrate, even the catalyst loading reduced to 1/5,000 (**1c**/ epichlorohydrin, mole ratio), admirable activity was obtained, yielding the chloropropene carbonate (**2e**) with a conversion of 98% in 8 h. Styrene oxide was also successfully transformed to styrene carbonate (**2f**) though compromised activity was observed, and the nucleophilic attack at both methine and methylene sites of styrene oxide was detected (Figure S14). Glycidol ethers could effectively form cyclic carbonates as evidenced by the use of butyl glycidyl ether, glycidyl ether, allyl glycidyl ether, and furyl glycidyl ether. Additionally, catalyst **1c** is also tolerant of alkene and hydroxyl functionalities, as noted by its ability to afford corresponding cyclic carbonates **2h**, **2i** and **2j** in 6 h with >98% conversions and >99% product selectivity. Cyclic bicarbonate (**2k**) was also effectively produced using resorcinol diglycidyl ether as the substrate in 6 h, at a catalyst loading of 0.2 mol%. Finally, more challenging substrates (internal epoxides) were used to test the catalytic ability. Though the reactivity was retarded, the epoxides can be successfully transformed into cyclic carbonate with > 99 % selectivity to cyclic carbonates (**2l**, **2m**, and **2n**). These efforts on broadening the substrate scope provide the generalization of our catalysts.

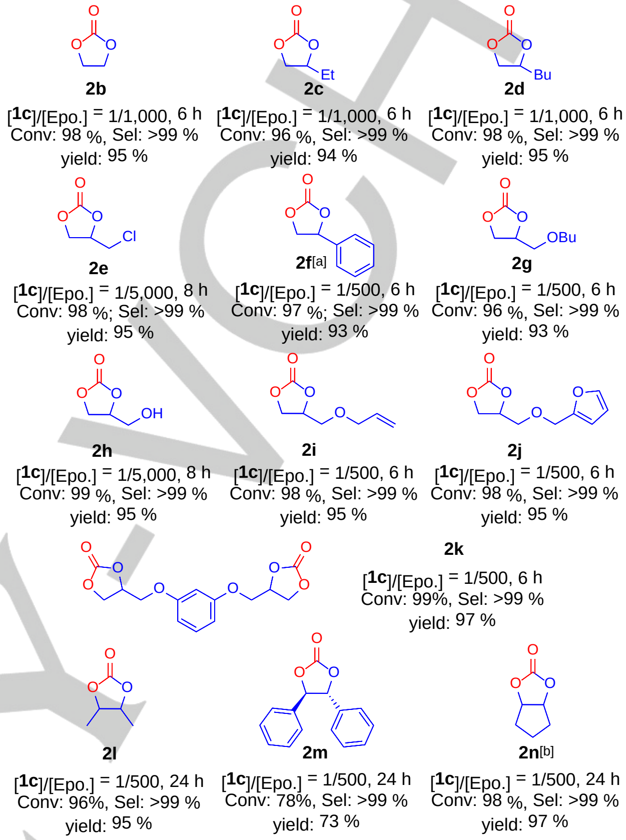

2b
[**1c**]/[Epo.] = 1/1,000, 6 h
Conv: 98 %, Sel: >99 %
yield: 95 %

2c
[**1c**]/[Epo.] = 1/1,000, 6 h
Conv: 96 %, Sel: >99 %
yield: 94 %

2d
[**1c**]/[Epo.] = 1/1,000, 6 h
Conv: 98 %, Sel: >99 %
yield: 95 %

2e
[**1c**]/[Epo.] = 1/5,000, 8 h
Conv: 98 %; Sel: >99 %
yield: 95 %

2f[a]
[**1c**]/[Epo.] = 1/500, 6 h
Conv: 97 %; Sel: >99 %
yield: 93 %

2g
[**1c**]/[Epo.] = 1/500, 6 h
Conv: 96 %, Sel: >99 %
yield: 93 %

2h
[**1c**]/[Epo.] = 1/5,000, 8 h
Conv: 99 %, Sel: >99 %
yield: 95 %

2i
[**1c**]/[Epo.] = 1/500, 6 h
Conv: 98 %, Sel: >99 %
yield: 95 %

2j
[**1c**]/[Epo.] = 1/500, 6 h
Conv: 98 %, Sel: >99 %
yield: 95 %

2k
[**1c**]/[Epo.] = 1/500, 6 h
Conv: 99%, Sel: >99 %
yield: 97 %

2l
[**1c**]/[Epo.] = 1/500, 24 h
Conv: 96%, Sel: >99 %
yield: 95 %

2m
[**1c**]/[Epo.] = 1/500, 24 h
Conv: 78%, Sel: >99 %
yield: 73 %

2n[b]
[**1c**]/[Epo.] = 1/500, 24 h
Conv: 98 %, Sel: >99 %
yield: 97 %

Figure 5. Synthesis of cyclic carbonates from various epoxides and CO_2 by using **1c**. General conditions: neat epoxide, 2.0 g of substrate, 120 °C, 20 bar initial CO_2 pressure. [a] The reaction was conducted at 150 ^oC. [b] The reaction was conducted at 90 ^oC Epo., epoxide. The pure cyclic carbonate product was isolated by a column chromatography.

Conclusion

In summary, we show our efforts on cycloaddition of epoxides with CO_2 into various cyclic carbonates by using a kind of scalable organoboron catalysts. The catalysts are highly active towards a wide scope of cyclic carbonates, and can withstand a high temperature up to 150 ^oC, rendering our organoboron catalysts to be one of the most efficient metal-free catalytic systems to date. Compared with the current metal-free catalytic systems involved using mol% catalyst loading, the catalytic capacity of our catalyst was enhanced by three orders of magnitude (as high as 200,000/1 of epoxide/catalyst, mole ratio). This performance greatly narrows the gap between the metal-free catalysts and the state-of-the-art metallic compounds. The structure-performance relationship of the catalyst was systematically investigated. On the basis of the kinetic studies and key reaction intermediates, a detailed catalytic cycle was rationally proposed. We hope this work may inspire the areas of chemical conversions that are mainly based on the application of nucleophiles/electrophiles or Lewis acids/bases, such as Lewis pair chemistry.

Acknowledgements

This work was supported by the National Natural Science Foundation of China (Grants 91956123, 21802030, 51973186, and 21674090).

Conflict of interest

The authors declare no conflict of interest.

Keywords: CO_2 capture • Cyclic carbonate • Metal-free • Catalysis • Cooperative mechanism

References

[1] a) W. D. Jones, *J. Am. Chem. Soc.* **2020**, *142*, 4955–4957; b) J. Artz, T. E. Muller, K. Thenert, J. Kleinekorte, R. Meys, A. Sternberg, A. Bardow, W. Leitner, *Chem. Rev.* **2018**, *118*, 434−504; c) A. M. Appel, J. E. Bercaw, A. B. Bocarsly, H. Dobbek, D. L. DuBois, M. Dupuis, J. G. Ferry, E. Fujita, R. Hille, P. J. Kenis, C. A. Kerfeld, R. H. Morris, C. H. Peden, A. R. Portis, S. W. Ragsdale, T. B. Rauchfuss, J. N. Reek, L. C. Seefeldt, R. K. Thauer, G. L. Waldrop, *Chem. Rev.* **2013**, *113*, 6621−6658; d) P. Gao, S. Li, X. Bu, S. Dang, Z. Liu, H. Wang, L. Zhong, M. Qiu, C. Yang, J. Cai, W. Wei, Y. Sun, *Nat. Chem.* **2017**, *9*, 1019−1024.

[2] a) S. Kar, A. Goeppert, G. K. S. Prakash, *Acc. Chem. Res.* **2019**, *52*, 2892−2903; b) K. Sordakis, C. Tang, L. K. Vogt, H. Junge, P. J. Dyson, M. Beller, G. Laurenczy, *Chem. Rev.* **2018**, *118*, 372−433; c) Y. Y. Birdja, E. Pérez-Gallent, M. C. Figueiredo, A. J. Göttle, F. Calle-Vallejo, M. T. M. Koper, *Nat. Energy* **2019**, *4*, 732–745.

[3] a) X.-B. Lu, D. J. Darensbourg, *Chem. Soc. Rev.* **2012**, *41*, 1462−1484; b) A. J. Kamphuis, F. Picchioni, P. P. Pescarmona, *Green Chem.* **2019**, *21*, 406−448; c) X. Jin, J. Ding, Q. Xia, G. Zhang, C. Yang, J. Shen, B. Subramaniam, R. V. Chaudhari, *J. CO_2 Util.* **2019**, *34*, 115–148; d) F. D. Bobbink, A. P. van Muyden, P. J. Dyson, *Chem. Commun.* **2019**, *55*, 1360−1373; e) R. R. Shaikh, S. Pornpraprom, V. D'Elia, *ACS Catal.* **2018**, *8*, 419−450; f) J. W. Comerford, I. D. V. Ingram, M. North, X. Wu, *Green Chem.* **2015**, *17*, 1966–1987; g) M. Cokoja, C. Bruckmeier, B. Rieger, W. A. Herrmann, F. E. Kuhn, *Angew. Chem. Int. Ed.* **2011**, *50*, 8510–8537; *Angew. Chem.* **2011***, 123,* 8662−8690; h) A. Decortes, A. M. Castilla, A. W. Kleij, *Angew. Chem. Int. Ed.* **2010**, *49*, 9822−9837; *Angew.Chem.* **2010**, 122, 10016−10032; i) M. Liu, X. Wang, Y. Jiang, J. Sun, M. Arai, *Catal. Rev.: Sci. Eng.* **2018**, *61*, 214–269; j) Q.-W. Song, Z.-H. Zhou, L.-N. He, *Green Chem.* **2017**, *19*, 3707–3728; k) C. Miceli, J. Rintjema, E. Martin, E. C. Escudero-Adán, C. Zonta, G. Licini, A. W. Kleij, *ACS Catal.* **2017**, *7*, 2367–2373; l) L. Longwitz, J. Steinbauer, A. Spannenberg, T. Werner, *ACS Catal.* **2018**, *8*, 665–672; m) J. Steinbauer, A. Spannenberg, T. Werner, *Green Chem.* **2017**, *19*, 3769–3779; n) Y. Hu, J. Steinbauer, V. Stefanow, A. Spannenberg, T. Werner, *ACS Sustainable Chem. Eng.* **2019**, *7*, 13257–13269; o) R. Huang, J. Rintjema, J. González-Fabra, E. Martín, E. C. Escudero-Adán, C. Bo, A. Urakawa, A. W. Kleij, *Nat. Catal*. **2018**, *2*, 62−70.

[4] B. Schaffner, F. Schaffner, S. P. Verevkin, A. Borner, *Chem. Rev.* **2010**, *110*, 4554−4581.

[5] K. Xu, *Chem. Rev.* **2004**, *104*, 4303−4418.

[6] V. Besse, F. Camara, C. Voirin, R. Auvergne, S. Caillol, B. Boutevin, *Polym. Chem.* **2013**, *4*, 4545−4561.

[7] A. Cai, W. Guo, L. Martinez-Rodriguez, A. W. Kleij, *J. Am. Chem. Soc.* **2016**, *138*, 14194−14197.

[8] a) R. L. Paddock, S. T. Nguyen, *J. Am. Chem. Soc.* **2001**, *123*, 11498–11499; b) C. J. Whiteoak, N. Kielland, V. Laserna, E. C. Escudero-Adan, E. Martin, A. W. Kleij, *J. Am. Chem. Soc.* **2013**, *135*, 1228−1231; c) X.-B. Lu, B. Liang, Y.-J. Zhang, Y.-Z. Tian, Y.-M. Wang, C.-X. Bai, H. Wang, R. Zhang, *J. Am. Chem. Soc.* **2004**, *126*, 3732−3733; d) C. Martín, G. Fiorani, A. W. Kleij, *ACS Catal.* **2015**, *5*, 1353−1370; e) U. Bayer, D. Werner, C. Maichle-Mossmer, R. Anwander, *Angew. Chem. Int. Ed.* **2020**, *59*, 5830−5836; *Angew. Chem.* **2020**, *132*, 5879–5885; f) F. Della Monica, B. Maity, T. Pehl, A. Buonerba, A. De Nisi, M. Monari, A. Grassi, B. Rieger, L. Cavallo, C. Capacchione, *ACS Catal.* **2018**, *8*, 6882–6893; g) K. Yamaguchi, K. Ebitani, T. Yoshida, H. Yoshida, K. Kaneda, *J. Am. Chem. Soc.* **1999**, *121*, 4526−4527; h) J.-P. Cao, Y.-S. Xue, N.-F. Li, J.-J. Gong, R.-K. Kang, Y. Xu, *J. Am. Chem. Soc.* **2019**, *141*, 19487−19497; i) R. Babu, A. C. Kathalikkattil, R. Roshan, J. Tharun, D.-W. Kim, D.-W. Park, *Green Chem.* **2016**, *18*, 232–242; j) T. Ema, Y. Miyazaki, J. Shimonishi, C. Maeda, J. Y. Hasegawa, *J. Am. Chem. Soc.* **2014**, *136*, 15270−15279; k) D. Tian, B. Liu, Q. Gan, H. Li, D. J. Darensbourg, *ACS Catal.* **2012**, *2*, 2029−2035; l) W.-M. Ren, Y. Liu, X.-B. Lu, *J. Org. Chem.* **2014**, *79*, 9771−9777; m) C. Maeda, T. Taniguchi, K. Ogawa, T. Ema, *Angew. Chem. Int. Ed.* **2015**, *54*, 134−138; *Angew. Chem.* **2015**, *127*, 136−140; n) K. Takaishi, B. D. Nath, Y. Yamada, H. Kosugi, T. Ema, *Angew. Chem. Int. Ed.* **2019**, *58*, 9984−9988; *Angew. Chem.* **2019**, *131*, 10089–10093; o) Y. Qin, H. Guo, X. Sheng, X. Wang, F. Wang, *Green Chem.* **2015**, *17*, 2853–2858; p) T. Ema, Y. Miyazaki, S. Koyama, Y. Yano, T. Sakai, *Chem. Commun.* **2012**, *48*, 4489–4491; q) J. Rintjema, A. W. Kleij, ChemSusChem **2017**, *10*, 1274–1282.

[9] a) H. Büttner, L. Longwitz, J. Steinbauer, C. Wulf, T. Werner, *Top. Curr. Chem.* **2017**, *375*, 50; b) M. Cokoja, M. E. Wilhelm, M. H. Anthofer, W. A. Herrmann, F. E. Kuhn, *ChemSusChem* **2015**, *8*, 2436−2454; c) M. Alves, B. Grignard, R. Mereau, C. Jerome, T. Tassaing, C. Detrembleur, *Catal. Sci. Technol.* **2017**, *7*, 2651−2684.

[10] a) F. D. Bobbink, D. Vasilyev, M. Hulla, S. Chamam, F. Menoud, G. b. Laurenczy, S. Katsyuba, P. J. Dyson, *ACS Catal.* **2018**, *8*, 2589−2594; b) M. H. Anthofer, M. E. Wilhelm, M. Cokoja, I. I. Markovits, A. Pöthig, J. Mink, W. A. Herrmann, F. E. Kühn, *Catal. Sci. Technol.* **2014**, *4*, 1749−1758; c) W.-L. Dai, B. Jin, S.-L. Luo, X.-B. Luo, X.-M. Tu, C.-T. Au, *J. Mol. Catal. A: Chem.* **2013**, *378*, 326−332; d) J. Hu, H. Liu, B. Han, *Sci. China Chem.* **2018**, *61*, 1486–1493.

[11] a) V. Calo, A. Nacci, A. Monopoli, A. Fanizzi, *Org. Lett.* **2002**, *4*, 2561–2563; b) Y. Kumatabara, M. Okada, S. Shirakawa, *ACS Sustainable Chem. Eng.* **2017**, *5*, 7295−7301; c) T. Ema, K. Fukuhara, T. Sakai, M. Ohbo, F.-Q. Bai, J.-y. Hasegawa, *Catal. Sci. Technol.* **2015**, *5*, 2314−2321; d) X. Meng, H. He, Y. Nie, X. Zhang, S. Zhang, J. Wang, *ACS Sustainable Chem. Eng.* **2017**, *5*, 3081−3086; e) M. Liu, X. Li, L. Liang, J. Sun, *J. CO_2 Util.* **2016**, *16*, 384−390; f) H. Büttner, K. Lau, A. Spannenberg, T. Werner, *ChemCatChem* **2015**, *7*, 459−467; g) K. Y. Yoshihiro Tsutsumi, Masahiko Yoshida, Tadashi Ema, and Takashi Sakai, *Org. Lett.* **2010**, *12*, 5728−5731.

[12] a) Y. Toda, Y. Komiyama, A. Kikuchi, H. Suga, *ACS Catal.* **2016**, *6*, 6906−6910; b) S. Liu, N. Suematsu, K. Maruoka, S. Shirakawa, *Green Chem.* **2016**, *18*, 4611−4615; c) B. Chatelet, L. Joucla, J. P. Dutasta, A. Martinez, K. C. Szeto, V. Dufaud, *J. Am. Chem. Soc.* **2013**, *135*, 5348−5351; d) G. Yuan, Y. Zhao, Y. Wu, R. Li, Y. Chen, D. Xu, Z. Liu, *Sci. China Chem.* **2017**, *60*, 958−963; e) T. Werner, H. Büttner, *ChemSusChem* **2014**, *7*, 3268−3271; f) J. Großeheilmann, H. Büttner, C. Kohrt, U. Kragl, T. Werner, *ACS Sustainable Chem. Eng.* **2015**, *3*, 2817−2822; g) H. Zhou, G.-X. Wang, W.-Z. Zhang, X.-B. Lu, *ACS Catal.* **2015**, *5*, 6773−6779.

[13] a) N. Fanjul-Mosteirín, C. Jehanno, F. Ruipérez, H. Sardon, A. P. Dove, *ACS Sustainable Chem. Eng.* **2019**, *7*, 10633–10640; b) X. Meng, Z. Ju, S. Zhang, X. Liang, N. von Solms, X. Zhang, X. Zhang, *Green Chem.* **2019**, *21*, 3456–3463; c) T. Yu, R. G. Weiss, *Green Chem.* **2012**, *14*, 209–216.

[14] W. Desens, T. Werner, *Adv. Synth. Catal.* **2016**, *358*, 622–630.

[15] a) S. Arayachukiat, C. Kongtes, A. Barthel, S. V. C. Vummaleti, A. Poater, S. Wannakao, L. Cavallo, V. D'Elia, *ACS Sustainable Chem.*

Eng. **2017**, *5*, 6392−6397; b) S. Sopeña, E. Martin, E. C. Escudero-Adán, A. W. Kleij, *ACS Catal.* **2017**, *7*, 3532−3539; c) T. Wang, D. Zheng, J. Zhang, B. Fan, Y. Ma, T. Ren, L. Wang, J. Zhang, *ACS Sustainable Chem. Eng.* **2017**, *6*, 2574−2582; d) M. Liu, P. Zhao, Y. Gu, R. Ping, J. Gao, F. Liu, *J. CO_2 Util.* **2020**, *37*, 39−44; e) X.-F. Liu, Q.-W. Song, S. Zhang, L.-N. He, *Catal. Today* **2016**, *263*, 69−74; f) C. J. Whiteoak, A. Nova, F. Maseras, A. W. Kleij, *ChemSusChem* **2012**, *5*, 2032−2038; g) M. Alves, B. Grignard, S. Gennen, R. Mereau, C. Detrembleur, C. Jerome, T. Tassaing, *Catal. Sci. Technol.* **2015**, *5*, 4636−4643; h) X. Wu, C. Chen, Z. Guo, M. North, A. C. Whitwood, *ACS Catal.* **2019**, *9*, 1895−1906; i) N. Liu, Y.-F. Xie, C. Wang, S.-J. Li, D. Wei, M. Li, B. Dai, *ACS Catal.* **2018**, *8*, 9945−9957; j) L. Martinez-Rodriguez, J. Otalora Garmilla, A. W. Kleij, *ChemSusChem* **2016**, *9*, 749−755; k) T. Ema, M. Yokoyama, S. Watanabe, S. Sasaki, H. Ota, K. Takaishi, *Org. Lett.* **2017**, *19*, 4070−4073.

[16] a) S. Subramanian, J. Oppenheim, D. Kim, T. S. Nguyen, W. M. H. Silo, B. Kim, W. A. Goddard, C. T. Yavuz, *Chem* **2019**, *5*, 3232−3242; b) T. S. Nguyen, C. T. Yavuz, *Chem. Commun.* **2020**, *56*, 4273−4275; c) Y. Liu, W. Cheng, Y. Zhang, J. Sun, S. Zhang, *Green Chem.* **2017**, *19*, 2184–2193; d) Y. A. Alassmy, Z. Asgar Pour, P. P. Pescarmona, *ACS Sustainable Chem. Eng.* **2020**, *8*, 7993−8003.

[17] G.-W. Yang, Y.-Y. Zhang, R. Xie, G.-P. Wu, *J. Am. Chem. Soc.* **2020**, *142*, 12245–12255.

[18] G.-W. Yang, Y.-Y. Zhang, R. Xie, G.-P. Wu, *Angew. Chem. Int. Ed.* **2020**, 10.1002/anie.202002815.

[19] K. A. Andrea, F. M. Kerton, *ACS Catal.* **2019**, 1799−1809.

[20] a) G.-P. Wu, S.-H. Wei, W.-M. Ren, X.-B. Lu, B. Li, Y.-P. Zu, D. J. Darensbourg, *Energy Environ. Sci.* **2011**, *4*, 5084−5092; b) X.-B. Lu, L. Shi, Y.-M. Wang, R. Zhang, Y.-J. Zhang, X.-J. Peng, Z.-C. Zhang, B. Li, *J. Am. Chem. Soc.* **2006**, *128*, 1664−1674; c) D. J. Darensbourg, S.-H. Wei, *Macromolecules* **2012**, *45*, 5916−5922.

[21] J. Burés, *Angew. Chem. Int. Ed.* **2016**, *55*, 2028−2031; *Angew.Chem.* **2016**, *128*, 2068–2071.

[22] N. Baser-Kirazli, R. A. Lalancette, F. Jäkle, *Angew. Chem. Int. Ed.* **2020**, *59*, 8689-8697; *Angew. Chem.* **2020**, *132*, 8767–8775.

Entry for the Table of Contents

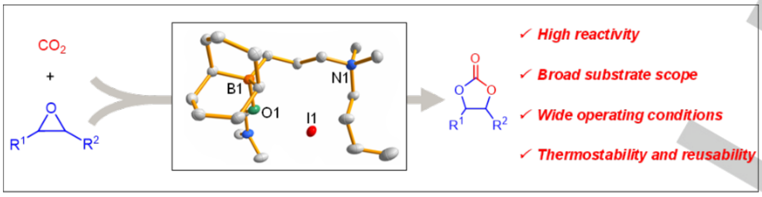

A kind of highly active bifunctional organoboron catalyst combined merits of scalable preparation, thermostability, and recyclability was reported for cyclization of CO_2 and epoxides. An intramolecular cooperative mechanism was proposed and substantiated by investigations on crystal structure of catalysts, structure-performance relationship, kinetic studies, and key reaction intermediates.